1

Ubiquitin-dependent folding of the Wnt signaling coreceptor LRP6

3

4

5 Elsa Perrody*[1], Laurence Abrami*[1], Michal Feldman[1], Beatrice Kunz[1], Sylvie Urbé[2] and F.

6 Gisou van der Goot[1,+]

7

8

9 *[1] Global Health Institute, Ecole Polytechnique Fédérale de Lausanne, Station 19, 1015*

10 *Lausanne, Switzerland; [2] Institute of Translational Medicine, University of Liverpool, UK*

11

12

13

14 ***Running title: Ubiquitin-dependent folding in the ER***

15

16

17 * Contributed equally to this work

18 [+] Corresponding author

19 Gisou van der Goot

20 Global Health Institute, EPFL, Station 19

21 CH 1015 Lausanne, Switzerland

22 Tel: (41) 021 693 1792

23 Fax: (41) 021 693 9538

24 E-mail: gisou.vandergoot@epfl.ch

25 **SUMMARY**

26 Many membrane proteins fold inefficiently and require the help of enzymes and chaperones.
27 Here we reveal a novel folding assistance system that operates on membrane proteins from the
28 cytosolic side of the endoplasmic reticulum (ER). We show that folding of the Wnt signaling
29 coreceptor LRP6 is promoted by ubiquitination of a specific lysine, retaining it in the ER
30 while avoiding degradation. Subsequent ER exit requires removal of ubiquitin from this lysine
31 by the deubiquitinating enzyme USP19. This ubiquitination-deubiquitination is conceptually
32 reminiscent of the glucosylation-deglucosylation occurring in the ER lumen during the
33 calnexin/calreticulin folding cycle. To avoid infinite futile cycles, folded LRP6 molecules
34 undergo palmitoylation and ER export, while unsuccessfully folded proteins are, with time,
35 polyubiquitinated on other lysines and targeted to degradation. This ubiquitin-dependent
36 folding system also controls the proteostasis of other membrane proteins as CFTR and anthrax
37 toxin receptor 2, two poor folders involved in severe human diseases.

38

39

40 **INTRODUCTION**

41 While protein folding may be extremely efficient, the presence of multiple domains, in soluble
42 or membrane proteins, greatly reduces the efficacy of the overall process. Thus, a set of
43 enzymes and chaperones assist folding and ensure that a sufficient number of active molecules
44 reach their final destination (Brodsky and Skach, 2011; Ellgaard et al., 2016). Even with help,
45 folding may remain inefficient and thereby sensitive to errors or mutations, leading to disease.
46 An illustrative example of folding inefficiency, and the consequences thereof, is the Cystic
47 Fibrosis Transmembrane Regulator (CFTR), a chloride channel expressed at the surface of
48 lung epithelial cells (Riordan, 2008). It has been estimated that less than 25% of newly
49 synthesized CFTR molecules actually reach the plasma membrane. When the number of
50 functional CFTR channels is further reduced, patients suffer from Cystic Fibrosis (Riordan,
51 2008). This is the case for mutations that affect the kinetics or thermodynamics of CFTR
52 folding in the ER, such as the most frequent CF mutation ΔF508, and which are recognized by
53 ER quality control systems and targeted for degradation (Riordan, 2008).

54 Inefficiency in folding is a fairly common characteristic of transmembrane proteins (Abrami et
55 al., 2008b; Deuquet et al., 2009; Guerriero and Brodsky, 2012). Most transmembrane proteins,
56 which jointly compose 30% of the human proteome, are synthesized by ER-bound ribosomes
57 and co-translationally inserted into the ER membrane (Ellgaard et al., 2016; Xu and Ng,
58 2015). Subsequent folding must proceed in three topological environments: the ER lumen, the
59 membrane and the cytosol. In each of these environments, the protein may benefit from the
60 help of chaperones and folding enzymes. On the luminal side, these are fairly well
61 characterized and include HSP40, HSP70 and HSP90 family members (Brodsky and Skach,
62 2011), the lectin chaperones calnexin and calreticulin (Lamriben et al., 2016) and protein

63 disulfide isomerases (Brodsky and Skach, 2011). Less is known about the assisted folding in
64 the ER membrane and on the cytosolic side. If folding or assembly in any of these
65 environments fails, the protein is recognized by quality control machineries and targeted to the
66 ER associated degradation (ERAD) pathway (Lemus and Goder, 2014). ERAD involves
67 polyubiquitination of the cytosolic domains of transmembrane protein, extraction from the ER
68 membrane and degradation by the proteasome (Lemus and Goder, 2014).
69 Here we have studied the biogenesis of Low-density lipoprotein Receptor-related Protein 6
70 (LRP6), a key component of the canonical Wnt signaling pathway, which has been associated
71 with many human pathologies including cancer, osteoporosis and metabolic diseases (Joiner et
72 al., 2013), but also involved in the formation of gap junctions in cardiomyocytes (Li et al.,
73 2016). LRP6 is a type I membrane protein composed of a large extracellular domain
74 containing multiple ß-propeller and EGF-like domains (MacDonald et al., 2009). Proper
75 folding of the ß-propeller domains depends of the dedicated LRP6 chaperone Mesd
76 (mesoderm development) (Hsieh et al., 2003) and possibly other chaperones such as calnexin.
77 We have previously shown that exit of LRP6 from the ER also requires a cytoplasmic post-
78 translational modification, namely S-palmitoylation, on two cysteine residues in close
79 proximity to the transmembrane domain (Abrami et al., 2008b). LRP6 acylation influences the
80 conformation of this domain, possibly by alleviating the hydrophobic mismatch between the
81 thickness of the membrane and the length of the hydrophobic stretch composing the
82 transmembrane domain. Mutation of the palmitoylation sites leads to retention of LRP6 in the
83 ER and ubiquitination on Lys-1403 (Abrami et al., 2008b) indicative of its recognition by a
84 quality control mechanism (Feldman and van der Goot, 2009). Once properly folded, LRP6
85 exits the ER, it transits through the Golgi, as indicated by the acquisition of Endoglycosidase

86 H insensitive complex sugars (Abrami et al., 2008b), before reaching the plasma membrane
87 where its signal role takes place.
88 Here we have further investigated LRP6 biogenesis in the ER. We show that newly
89 synthesized wild type LRP6 also undergoes ubiquitination, on the same site (Lys-1403), and
90 that this post-translational modification promotes its folding. For ER exit to occur,
91 ubiquitination must however be subsequently removed. This is mediated by the
92 deubiquitinating enzyme USP19, one of the isoforms of which is tail-anchored to the ER
93 (Hassink et al., 2009; Wing, 2016). It is thought to play an essential role in skeletal muscle
94 atrophy through unclear mechanisms (Wing, 2016). At the more mechanistic level, USP19 has
95 been shown to control the stability of several cytoplasmic proteins such as the inhibitors of
96 apoptosis c-IAP1, and c-IAP2 (Mei et al., 2011), hypoxia-inducible factor 1-alpha (HIF-1α)
97 (Altun et al., 2012) and the initiator of autophagy Beclin1 (Jin et al., 2016). Interestingly,
98 USP19 is a target gene of the unfolded protein response (UPR) and was found to rescue CFTR
99 ΔF508 from ERAD (Hassink et al., 2009). More recently it was found that USP19 is a key
100 player in a novel misfolded-protein associated secretion MAPS pathway (Lee et al., 2016). We
101 show that USP19 controls the cellular levels of LRP6. In the absence of USP19, LRP6 is
102 efficiently targeted to ERAD. Upon USP19 overexpression, ER exit of LRP6 is greatly
103 enhanced.
104 This work reveals the existence of a novel assisted-folding system that operates on the
105 cytosolic side of the ER and depends on site-specific cycles of ubiquitination-deubiquitination.
106 Upon ubiquitination on Lys-1403, LRP6 presumably interacts with an ubiquitin-binding
107 protein that acts as a chaperone and provides the protein with time to fold. If folding is
108 successful, LRP6 is transported out of the ER, a step that is favored by palmitoylation (Abrami

109 et al., 2008b). If folding is impaired or delayed, polyubiquitination of other cytosolic lysine
110 residues takes over and targets LRP6 to ERAD. The here identified ubiquitination-
111 deubiquitination assisted-folding cycle also appears to operate on other membrane proteins
112 such as CFTR or the anthrax toxin receptor 2 (also know as Capillary Morphogenesis gene 2,
113 CMG2), loss of function of which leads to Hyaline Fibromatosis Syndrome (Deuquet et al.,
114 2011b).

115

116 **RESULTS AND DISCUSSION**

117 **Massive degradation of newly synthesized LRP6 in the ER**

118 We analyzed LRP6 stability by performing a cycloheximide chase, which consists in
119 following total protein expression levels by western blot analysis of extracts from Pigmented
120 epithelial (RPE1) cells submitted for various times to a protein synthesis block. No significant
121 decay of LRP6 was observed over a 6hrs period (fig. 1AB). We next measured LRP6 stability
122 by performing ^{35}S Cys/Met metabolic pulse-chase experiments. Protein decay, monitored
123 following a 20 min metabolic pulse, indicated that the apparent half-life ($t_{\frac{1}{2}}^{app}$) of endogenous
124 LRP6 in RPE1 cells is approximately 3 hrs (Fig. 1CD, and supplementary information in
125 (Abrami et al., 2008b)). The same experiment was repeated on transiently expressed myc-
126 LRP6 in HeLa cells (Fig. 1-figure supplement 1). Then, we show that $t_{\frac{1}{2}}^{app}$ was identical for
127 endogenous LRP6 in RPE1 cells and transiently expressed myc-LRP6 in Hela, indicating that
128 the potential difference in expression in these two systems does not affect degradation rates
129 and allowing us to use both systems.
130 The above apparent discrepancy between the cycloheximide chase and the metabolic labeling
131 approach is due to the fact that stability of mature LRP6 is monitored through the first

132 approach, while newly synthesized LRP6 is monitored by the second. Considering the events
133 that occur following synthesis of a membrane protein –more or less efficient folding, ER exit,
134 transport to destination–, the $t_{\frac{1}{2}}^{app}$ of a protein determined using metabolic pulse-chase
135 experiments may greatly dependent on the duration of the pulse. Indeed, the $t_{\frac{1}{2}}^{app}$ of LRP6
136 increased to ≈ 5hrs for a 2 hrs pulse and >15 hrs for a 16 hrs pulse (Fig. 1CDE). The long
137 apparent half-lives estimated both by long metabolic labeling and cycloheximide chase
138 suggest that mature LRP6 has a half-life that exceeds 20 hrs. The rapid decay times observed
139 for short metabolic pulses on the other hand indicate that close to 80% of newly synthesized
140 LRP6 molecules are degraded in our cells within the first 6 hrs (Fig. 1D), and thus do not
141 contribute to the population of active Wnt signaling co-receptors.
142 Cellular degradation of membrane proteins can occur by two main pathways: ERAD, where
143 proteolysis is mediated by the proteasome, or the lysosomal pathway, which is responsible for
144 degradation of most membrane proteins but is also the endpoint of autophagy (Fig. 1I). To
145 determine the relative contribution of these pathways to the degradation of LRP6, we repeated
146 the 20 min metabolic pulse-chase experiments while either inhibiting the proteasome with
147 MG132 or preventing lysosomal degradation by inhibiting the vacuolar ATPase with
148 Bafilomycin A. MG132 protected LRP6 from degradation early after synthesis (Fig. 1FG),
149 consistent with degradation of a subpopulation of LRP6 molecules by ERAD during
150 biogenesis. Bafilomycin A protected LRP6 at later times (Fig. 1FG), consistent with transport
151 of a portion of newly synthesized LRP6 molecules to the plasma membrane and their
152 subsequent endocytosis and targeting to lysosomes (Fig. 1I). That LRP6 undergoes
153 degradation by two distinct pathways is further support by the observation that palmitoylation
154 deficient LRP6, in which the two cysteines are mutated to serines ($LRP6^{CC-SS}$), and which

155 does not exit the ER (Abrami et al., 2008b), is partially rescued by MG132 (Fig. 1H) but is
156 insensitive to inhibitors of lysosomal enzymes such as Bafilomycin A (Fig. 1H) or leupeptin
157 (supplementary information in (Abrami et al., 2008b)). The involvement of lysosomal
158 enzymes in LRP6 degradation thus requires export out of the ER.
159

160 **Role of palmitoylation and ubiquitination in LRP6 biogenesis**

161 We have previously shown that LRP6 undergoes palmitoylation in the ER on Cys-1394 and
162 Cys-1399 and that palmitoylation is required for ER exit (Abrami et al., 2008b). This was
163 based on the observation that palmitoylation deficient LRP6 did not exit the ER and
164 underwent ubiquitination on Lys-1403 (Abrami et al., 2008b). To further investigate the
165 importance of palmitoylation and ubiquitination on LRP6 biogenesis, we performed ^{35}S
166 Cys/Met metabolic pulse-chase experiments on the palmitoylation deficient $\mathrm{LRP6}^{\mathrm{CC-SS}}$
167 mutant, on the K1403R mutant ($\mathrm{LRP6}_{\mathrm{K1403R}}$) and on the triple mutant ($\mathrm{LRP6}_{\mathrm{K1403R}}^{\mathrm{CC-SS}}$).
168 Following a 20 min pulse, no significant difference in degradation was observed between wild
169 type LRP6 and $\mathrm{LRP6}^{\mathrm{CC-SS}}$ (Fig. 2A) in agreement with our previous observations (Abrami et
170 al., 2008b). In contrast, degradation was accelerated by the K1403R mutation (Fig. 2A).
171 To estimate the importance of the contribution of Lys-1403 to LRP6 folding, we compared the
172 effect of this mutation to that of silencing the dedicated LRP6 chaperone Mesd. Remarkably,
173 mutation of Lys-1403 had a more pronounced effect on LRP6 degradation than *mesd* silencing
174 (Fig. 2B). Accelerated $\mathrm{LRP6}_{\mathrm{K1403R}}$ degradation did not involve lysosomes since Bafilomycin
175 A had no effect, also suggesting that newly synthesized $\mathrm{LRP6}_{\mathrm{K1403R}}$ does not significantly exit
176 the ER during the 6 hrs that follow its synthesis. Degradation of $\mathrm{LRP6}_{\mathrm{K1403R}}$ could however
177 be partially rescued by MG132 (Fig. 2C).

178 Consistent with its targeting to the proteasome, $LRP6_{K1403R}$underwent polyubiquitination as
179 revealed when immunoprecipitating LRP6 from MG132 treated cells and blotting against
180 ubiquitin (Fig. 2D). This observation also shows that ERAD targeting of LRP6 does not
181 involve, or at least does not require, Lys-1403 polyubiquitination.
182 Extending the pulse time to 2 or 16 hrs revealed that the stability of LRP6 does depend on
183 palmitoylation (Fig. 2EF). The tripple $LRP6_{K1403R}^{CC-SS}$ mutant was therefore the least stable (Fig.
184 2F).
185 Altogether these observations indicate that spontaneous folding of LRP6 is very inefficient,
186 and that both ubiquitination and palmitoylation promote LRP6 biogenesis and ER exit. The
187 process is however not all-or-none, *i.e.* even in the absence of Lys-1403 and/or palmitoylation,
188 a small population of molecules folds properly and exits the ER. Pulse-chase experiments with
189 long ^{35}S pulses indeed reveal biphasic decay curves for all mutants studied, and show the
190 existence, irrespective of the mutations, of a minor population of extremely long-lived
191 molecules, which presumably reside at the plasma membrane. Importantly these constitute the
192 steady state population that is revealed by western blotting. Western blot analysis of LRP6
193 mutants may therefore be misleading as to the importance of specific residues for biogenesis
194 and membrane targeting (Abrami et al., 2008b).
195
196 **Working Hypothesis**
197 The above findings, combined with our previous observation that $LRP6^{CC-SS}$ undergoes
198 ubiquitination on Lys-1403 and fails to exit the ER (Abrami et al., 2008b), led us to propose
199 the following working hypothesis: following synthesis and insertion into the ER membrane,
200 LRP6 first undergoes ubiquitination, probably of a specific type, on Lys-1403, allowing it to

201 interact with an ER or cytosolic ubiquitin-binding protein. This interaction provides LRP6
202 with time to fold –and as such this ubiquitin-binding protein would act as a chaperone–
203 protecting it from ERAD targeting. Lys-1403 is then deubiquitinated. At this stage, LRP6 can
204 either 1) undergo palmitoylation of its two juxtamembranous cysteine residues, followed by
205 ER exit, 2) be re-ubiquitinated on Lys-1403, or 3) be polyubiquitinated on one of the other 16
206 cytoplasmic lysine residues and sent to ERAD. Option 1, re-ubiquitination on Lys-1403,
207 allows LRP6 to undergo a second cycle of interaction with its ubiquitin-binding chaperone,
208 further promoting folding. Palmitoylation, which favors ER exit (Abrami et al., 2008b), could
209 prevent LRP6 from Lys-1403 ubiquitination, possibly through a conformational change of
210 steric hindrance given the juxtamembrane localization of both modifications.
211 A major prediction of this model is the existence of an ER localized deubiquitinating (DUB)
212 enzyme that can remove ubiquitin specifically from Lys-1403. This DUB would control LRP6
213 biogenesis.
214

215 **USP19 promotes LRP6 biogenesis and controls Wnt signaling**

216 The human genome encodes some 100 DUBs (Clague et al., 2013). Of these, the ubiquitin-
217 specific proteases (USPs) represent the largest family with 56 members (Ye, 2006). Because
218 LRP6 folding takes place in the ER, we searched for ER-associated DUBs and to the best of
219 our knowledge, only USP19 has an ER localized isoform (Clague et al., 2013; Hassink et al.,
220 2009; Wing, 2016). Endogenous LRP6 and USP19 could be co-immunoprecipitated from
221 RPE1 cells (Fig. 3A). While ubiquitination of LRP6 is undetectable under control condition
222 (Fig. 3A; see also (Abrami et al., 2008b)), silencing of *usp19* (Fig. 3-figure supplement 1A)
223 revealed a clear LRP6 ubiquitination signal (Fig. 3A), often, but not always, appearing as a
224 well identifiable band and a smear. Strikingly, LRP6 levels dropped drastically upon *usp19*

225 silencing whether in HeLa (Fig. 3-figure supplement 1B), RPE1 cells or primary human
226 fibroblasts (Fig. 3B and Fig. 3-figure supplement 1C). The same was observed upon
227 CRISPR/Cas9-mediated *usp19* knockout in RPE1 cells (Fig. 1-figure supplement 1B).
228 Silencing of *usp19* also led to an increase in ubiquitination of palmitoylation-deficient
229 $LRP6^{CC-SS}$ and a decrease of its expression (Fig. 3-figure supplement 1D). In reverse, over
230 expression of wild type USP19, but not of its catalytically inactive mutant ($USP19^{C506S}$
231 (Hassink et al., 2009)) reduced ubiquitination of $LRP6^{CC-SS}$ (Fig. 3-figure supplement 1E),
232 indicating that USP19 influences LRP6 ubiquitination in a manner that depends on its DUB
233 activity. Thus consistent with our working hypothesis, an ER-localized DUB, USP19, controls
234 the expression of LRP6.

235 We next investigated whether USP19 indeed affects LRP6 biogenesis. siRNA-mediated
236 silencing of *usp19* in HeLa cells and *usp19* knock-out in RPE1 cells (Figure 1-figure
237 supplement 1B) both led to a strong decrease in $t_{\frac{1}{2}}^{app}$ of LRP6, droping from 3 to 1 h, as
238 monitored by ^{35}S Cys/Met metabolic pulse-chase experiments (Fig. 3C and Figure 1-figure
239 supplement 1A). Overexpression of wild type USP19 led to a marked increase in $t_{\frac{1}{2}}^{app}$ to
240 above 6 hrs, beyond the time frame of these experiments. Importantly, overexpression of
241 catalytically inactive $USP19^{C506S}$ had no effect. This not only shows that the catalytic activity
242 of USP19 is required, but the complete absence of rescue also indicates that USP19 does not
243 act as a chaperone, as proposed for the unconventional misfolded protein-associated secretion
244 MAPS pathway (Lee et al., 2016).

245 The palmitoylation deficient $LRP6^{CC-SS}$ was affected in a qualitatively similar manner:
246 silencing *usp19* decreased $t_{\frac{1}{2}}^{app}$ to less than 1 hr, while over expression of USP19 increased

247 $t_{\frac{1}{2}}^{app}$ to 6 hrs (Fig. 3D). Remarkably, silencing or overexpression of USP19 had no effect

248 whatsoever on $\mathrm{LRP6}_{K1403R}$ (Fig. 3E). Mutation of Lys-1403 similarly abolished the regulatory

249 effect of USP19 on $\mathrm{LRP6}^{\mathrm{CC-SS}}$, $LRP6_{K1403R}^{CC-SS}$ being insensitive to the cellular USP19 levels

250 (Fig. 3F). Altogether these experiments clearly point to Lys-1403 as the specific target site of

251 USP19, revealing the crucial role of this residue in preventing early LRP6 degradation. These

252 experiments also show that USP19, even when overexpressed, cannot reverse the

253 polyubiquination undergone by $LRP6_{K1403R}$ and thus ERAD targeting, further highlighting

254 the specificity of this DUB. Finally, these observations demonstrate that USP19 promotes the

255 biogenesis of LRP6, with only 18% of newly synthesized LRP6 molecules surviving beyond 6

256 hrs in the absence of USP19 and 60% surviving upon USP19 overexpression.

257 We finally tested the importance of USP19 for LRP6 function, as the co-receptor in Wnt

258 signaling. Overexpression of USP19 in HeLa cells lead to a 50% increase in the Wnt signaling

259 capacity (Fig. 4A), monitored using the TOPFLASH reporter assay (Abrami et al., 2008a).

260 Most strikingly, silencing of usp19, but not usp13, in RPE1 cells stably expressing 7xTCF-

261 FFluc directly activated by the TCF/-βcatenin complex led to a more than 80% drop in Wnt

262 signaling (Fig. 4B). In agreement, surface biotinylation showed that *usp19* silencing lead to a

263 drastic drop LRP6 at the cell surface (Fig. 4-figure supplement 1).

264

265 **Concluding remarks**

266 We here reveal the existence of an ubiquitin-dependent folding machinery, which operates on

267 the cytosolic side of the ER membrane (Fig. 4C). More specifically we show that following

268 synthesis, LRP6 undergoes ubiquitination on Lys-1403, most likely of a specific form. In

269 conceptual analogy to the binding of newly synthesized mono-glucosylated proteins to

270 calnexin in the ER lumen (Lamriben et al., 2016), we hypothesize that Lys-1403-ubiquitin can
271 interact with a putative ER-ubiquitin binding protein that would also act as a chaperone. Upon
272 release from this putative ubiquitin-binding chaperone, LRP6 is deubiquitinated by USP19.
273 Following USP19 deubiquitination, LRP6 can, if properly folded, exit the ER, an events
274 possibly promoted by palmitoylation of cysteines in the vicinity of Lys-1403 (Abrami et al.,
275 2008b). Or, LRP6 can undergo a new cycle of Lys-1403-specific ubiquitination and chaperone
276 binding. Upon prolonged presence in the ER, LRP6 undergoes polyubiquitination on other
277 cytosolic lysines, leading to ERAD targeting. In the ER, LRP6 can thus undergo two types of
278 ubiquitination events, which operate with different kinetics: 1) specific ubiquitination on Lys-
279 1403 which promotes folding, 2) the slower polyubiquitination on other lysines which
280 promotes ERAD. These two types of ubiquitination events are reminiscent of de-glucosidation
281 and de-mannosidation of glycoproteins in the ER lumen, which also occur with different
282 kinetics. De-glucosidation promotes folding of glycosylated protein, but if folding is too
283 lengthy or fails, de-mannosidation takes place and targets the protein to ERAD.
284 While the here described ubiquitin-dependent folding system was identified for LRP6, it likely
285 also operates on other membrane proteins. We indeed found that *usp19* silencing also led to a
286 pronounced decrease in the levels of CMG2 (Fig 4D), defective folding of which lead to
287 Hyaline Fibromatosis Syndrome (OMIM #228600) (Deuquet et al., 2009; Deuquet et al.,
288 2011a). Silencing of *usp19* however did not affect the levels of the CMG2-related protein
289 TEM8 (Tumor endothelial marker 8), nor those of the Transferrin and the EGF receptors (Fig
290 4D). USP19 was reported to rescue the CFTR Δ508 mutant, which is an ERAD substrate
291 (Hassink et al., 2009). USP19 however also controls proteostasis of wild type CFTR (Fig 4E).
292 Future studies are required to establish the generality of this ubiquitin-dependent folding

293 system, determine whether it has a built-in quality control, and identify the missing
294 components such as the folding-promoting ubiquitin ligase, the putative ubiquitin-binding
295 chaperone and the degradation-targeting ligase (Fig. 4C). All these enzymes could be
296 exploited to control Wnt signaling in the context of disease.
297

298 MATERIAL AND METHODS

299 *Cell Lines and Cell Culture*

300 Hela and RPE1 cells were used in this study. These cells are not on the list of commonly
301 misidentified cell lines maintained by the International Cell Line Authentication Committee .
302 They were mycoplasma negative as tested on a trimestral basis using the MycoProbe
303 Mycoplasma Detection Kit CUL001B. RPE1 cells were maintained in DMEM high glucose
304 supplemented with 10% Fetal Calf Serum, 2mM penicillin and Streptomycin and HeLa cells
305 were maintained in MEM supplemented with 10% FCS, 2mM L-Glutamine and antibiotics.
306 RPE1 USP19 knockout cell lines were generated using the CRISPR/Cas9 technology. Briefly,
307 the cells were co-transfected with three plasmids: MLML3636, JDS246 carrying the gRNA
308 sequence TCTGGCGGGGCCAGTGCCAC and GFP encoding plasmid. Single GFP
309 transfected cells were sorted by FACS in 96 well plates. The Knockout clones were detected
310 by western blot (Fig. S1B).
311

312 *Antibodies and Reagents*

313 We used the following primary antibodies: Rabbit anti-LRP6 mAb (Cell Signaling, #2560
314 RRID:AB_2139329), Mouse anti-Actin mAb (Millipore, MAB1510), Mouse anti-Myc 9E10
315 mAb (Covance MMS-150R RRID:AB_291327), Mouse Ubiquitin (Santa Cruz sc-8017
316 RRID:AB_628423), Goat anti-CMG2 (R&D systems #AF2940), TEM8 (Sigma

317 SAB2501028), Mouse anti-Tf-R (Zymed, #13-6800), Mouse anti-EGF-R (Sigma E3138,
318 RRID:AB_476925), CFTR (home-made), Mouse anti-Tubulin (Sigma T5168), Mouse anti-
319 GFP (Roche, #11814460001), Rabbit anti-USP19 (Bethyl, A301-587A, RRID:AB_1078839).
320 We used the following beads for immunoprecipitations: Protein G Sepharose 4 Fast Flow (GE
321 Healthcare, 17-0618-01), Streptavidin Agarose (Sigma, S1638), anti-Myc Affinity Gel
322 (Thermo Scientific # 20169).
323
324 *Plasmids and Transfections*
325 LRP6 encoding plasmids as been previously described (Abrami et al., 2008b). The
326 catalytically inactive mutant was obtained by Quik Change Technology (Agilent) according to
327 manufacturer's instruction. Plasmids were transfected into RPE1 and HeLa cells for 24h in
328 cDNA/9.6cm^2 plate using Fugene (Roche Diagnostics). For the dual Luciferase assay,
329 plasmids and reagents were from Promega.
330
331 *Biochemical assays*
332 For immunoprecipitation, cells were PBS washed and lysed 30min at 4°C in IP Buffer (0.5%
333 Nonidet P-40, 500 mM Tris pH 7.4, 20 mM EDTA, 10 mM NaF, 2 mM benzamidin and
334 protease inhibitor cocktail (Roche), and centrifuged 3-5 min at 5000 rpm. Supernatants were
335 incubated overnight with Sepharose beads. In case of non-coupled Sepharose G beads,
336 supernatants were subjected to preclearing with the beads prior to the actual
337 immunoprecipitation reaction.
338 Cell surface protein biotinylation was performed as described (Abrami et al., 2008b). Briefly,
339 silenced cells were treated 30 min with 0.17 mg/ml sulfo-NHS-Biotin (Pierce) at 4°C,
340 quenched with 100mM NH_4Cl, and lysed in IP Buffer (as described above). The lysate was

341 immunoprecipitated with streptavidin-coated sepharose beads (Sigma, S1638).

342 The dual luciferase assays were performed with plasmids and reagents from Promega.

343 HEK293 cells were transfected with 0.1ug TOP-Luciferase, 50 ng TK-Renilla, 0.25ug Mesd

344 encoding plasmid and 0.5 ug myc-LRP6 wild type or mutant encoding plasmids /9.6 cm^2

345 plate. The cells were lysed 24h after transfection and the luciferase activity was determined

346 according to the manufacturer's instructions.

347 The drugs are used in complete medium at the final concentration of 10 μM for MG132 and

348 100 nM for Bafilomycin A 2 hrs before the starvation and are kept during the whole

349 experiment.

350

351 *Metabolic and cycloheximide chases*

352 For the metabolic chases, the cells were starved in DMEM HG devoid of Cys/Met for 40

353 minutes at 37°C, pulsed with the same medium supplemented with 140 μCi of ^{35}S Cys/Met for

354 the indicated time, washed and incubated in DMEM complete medium for the indicated time

355 of chase (Abrami et al., 2008).

356 For the cycloheximide chases, the cells were incubated in medium supplemented with

357 10μg/ml of cycloheximide for 2 hours, washed and incubated in complete medium for the

358 indicated time.

359

360

361 **AUTHOR CONTRIBUTIONS**

362 Conceptualization, M.F., E.P., L.A., G.V.D.G.; Investigation, M.F., E.P., L.A., B.K.; Funding
363 Acquisition, G.V.D.G. Writing–Original Draft, M.F.; E.P., L.A., G.V.D.G.; Writing–Review
364 & Editing, S.U., B.K.; Resources, B. K., S.U., E.P.

365

366 **ACKNOWLEDGMENTS**

367 We are grateful to Maria Zaballa and Jérôme Bürgi for critical reading of the manuscript and
368 many discussions, to Christophe Fuerer for the constructs to perform Wnt signaling
369 measurements. The work received funding from the European Research Council under the
370 European Union's Seventh Framework Program (FP7/2007-2013) / ERC grant agreement n°
371 340260 PalmERa and from the Swiss National Science Foundation. M.F. was the recipient of
372 a long term EMBO fellowship.

373

374

375

376 **FIGURE LEGENDS**

377 **Figure 1: LRP6 undergoes rapid degradation following synthesis in the ER but is stable**
378 **once mature. A:** representative western blot of a cycloheximide (CHX) chase in RPE1 cells.
379 40 µg of total cell extracts from RPE1 cells were loaded per lane, analyzed by SDS-PAGE
380 followed by Western blotting against endogenous LRP6, calnexin (Calx), a stable protein and
381 Myc, a short lived protein. **B:** Experiments as in A were quantified by ImageJ software, n=3.
382 **CDE**: RPE1 cells were submitted to metabolic ^{35}S Cys/Met labeling for different times and
383 subsequently chased for different times. Endogenous LRP6 was immunoprecipitated with an
384 anti-LRP6 antibody. A representative experiment in shown in **C**. Autoradiograms were
385 quantified using the Typhoon imager and means of different experiments were calculated (**D**
386 **and E**). Error bars represent standard deviation (n=6 for the 20 min pulse; n=4 for the 2 hrs
387 and 16 hrs pulses). **FG**: RPE1 cells were treated or not with MG132 or Bafilomycin A and
388 subsequently submitted, in the presence or not of the drugs, to metabolic a 20 min ^{35}S-
389 Cys/Met pulse followed by different chase times. A representative experiment in shown in **F**.
390 Errors represent standard deviation (n=4 for MG132; n=3 for Bafilomycin A, BafA, the WT
391 control curve corresponds to that shown in Fig. 1D). **G**: Hela cells transiently expressing myc-
392 tagged palmitoylation deficient LRP6 (CC-SS) were submitted to metabolic ^{35}S Cys/Met
393 labeling for different times and subsequently chased for different times. LRP6 was
394 subsequently immunoprecipitated using an anti-myc antibody. Errors represent standard
395 deviation (n=3). H: Cartoon depicting the two major cellular degradation pathways for
396 membrane proteins: ERAD (blocked by MG132) and lysosomal pathway (blocked by
397 Bafilomycin A).
398

399 **Figure 2: Mutation of the palmitoylation sites and the Lys-1403 ubiquitination site**
400 **accelerate LRP6 targeting to ERAD.** **A**: Metabolic ^{35}SCys/Met pulse chase experiment (20
401 minutes pulse) on transiently expressed myc-LRP6 wild type (WT, curve corresponding to the
402 one in Fig. 1D), palmitoylation deficient (CC-SS, n=3) or K1403R (KR, n=6) mutants in HeLa
403 cells. **B:** Metabolic ^{35}SCys/Met pulse chase experiment (20 minutes pulse) on transiently
404 expressed myc-LRP6 wild type (WT, n=7), or K1403R (K1403R, n=7) mutant in HeLa cells
405 silenced or not for *mesd* gene (siRNA mesd, n=3). Errors represent standard
406 deviation,*<p=0.05 calculated between LRP6 WT and K1403R. **C:** Metabolic ^{35}SCys/Met
407 pulse chase experiment (20 minutes pulse) on transiently expressed myc-LRP6K1403R in
408 HeLa cells supplemented or not (n= 6, curve corresponding to the one in Fig. 2A) with
409 MG132 (K1403 + MG123, n=3) or Bafilomycin A (K1403 + BafA, n=3). **D:**
410 Immunoprecipitation of myc-tagged LRP6 Wild Type (WT) and K1403 mutant (KR) revealed
411 with anti-Ubiquitin antibody, with or without MG132 treatment. **E:** Metabolic ^{35}SCys/Met
412 pulse chase experiment (2 hrs pulse) on transiently expressed myc-LRP6 wild type (WT, n=4,
413 curve corresponding to the one in Fig. 1D) or palmitoylation deficient (CC-SS, n=3) in HeLa
414 cells. **F**: Metabolic ^{35}SCys/Met pulse chase experiment (16h pulse) on transiently expressed
415 myc-LRP6 wild type (WT, curve corresponding to the one in Fig. 1D), palmitoylation
416 deficient (CC-SS, n=3), K1403R (K1403R, n=3) or K1403R in the palmitoyl deficient
417 background (CC-SS + KR, n=3) mutants in HeLa cells.
418
419 **Figure 3: De-ubiquitination of LRP6 by USP19 on Lys-1403 promotes LRP6 biogenesis.**
420 **A:** Immunoprecipitation of endogenous LRP6 and **B:** cellular level in RPE1 cells upon *usp19*
421 silencing. **C/D/E/F**: Metabolic ^{35}SCys/Met pulse chase experiment (20 minutes pulse) on
422 transiently expressed myc-LRP6 wild type (WT), palmitoylation deficient mutant (CC-SS),

423 K1403R mutant (K1403R) or K1403R mutation in the palmitoyl deficient background (CC-SS
424 + KR) mutants in HeLa cells upon over expression of GFP-tagged USP19 (O.E. USP19) or
425 GFP-tagged USP19 catalytically inactive (O.E. USP19 C-S) or upon *usp19* gene silencing
426 (siRNA USP19). C: WT n=6, same as in Fig. 1D, other conditions n=3, D (CC-SS curve
427 corresponding to the one in figure 2A) and F: all conditions n=3, E: K1403R n=6, other
428 conditions n=3.
429
430 **Figure 4: USP19 controls the Wnt signaling capacity of the cell. A:** Wnt signaling
431 measured in HEK293 cells carrying the TOPFLASH reporter assay, transiently transfected for
432 the indicated constructs (n=5) **B**: Wnt signaling measured in RPE1 cells stably expressing
433 lentiviral vector possessing a 7xTCF-FFluc upon *usp19* or *usp13* silencing (n=4). **C:** Working
434 model (described in the text). **D:** cellular level of the indicated endogenous proteins in RPE1
435 cells upon *usp19* silencing (siRNA) or overexpression (O.E.) of GFP-tagged USP19. **E**:
436 cellular level of transiently co-transfected CFTR (constant amount) and GFP-tagged USP19
437 (increasing amount) in RPE1 cells.
438

439 **FIGURE SUPPLEMENT LEGENDS**

440 **Figure 1-figure supplement 1: Variation in USP19 cellular amount influences LRP6**
441 **degradation rates. A:** Metabolic ^{35}SCys/Met pulse chase experiment (20 minutes pulse) in
442 the following conditions: immunoprecipitation of myc-LPR6 in HeLa cells transiently
443 expressing myc-LRP6 wild type (WT) upon control silencing (HeLa si Ctrl, n=7) *vs. usp19*
444 silencing (HeLa + siRNA USP19, n=6) or upon co-overexpression of myc-LRP6 wild type
445 and wild type GFP-tagged USP19 (HeLa + OE USP19 WT, n=6) *vs.* catalytically inactive
446 GFP-tagged USP19 (HeLa + O.E. USP19 CS, n=6); immunoprecipitation of endogenous
447 LRP6 in RPE1 cells wild type (RPE1, n=4) *vs.* RPE1 knout-out cells for *usp19* gene (RPE1
448 delta USP19, n=3). **B:** Total cell extract of wild type RPE1 and RPE1 knout-out cells for
449 *usp19* gene revealed with USP19, LRP6 and Actin antibodies.

450

451 **Figure 3-figure supplement 1: Variation in USP19 cellular amount influences LRP6**
452 **ubiquitination state. A:** RT-PCR detecting usp19, usp13 and LRP6 mRNA expression level
453 upon silencing of *usp19* and *usp13* genes with specific RNAi. Errors represent standard
454 deviation. **B:** Total cell extracts of Hela transiently expressing Myc-LRP6 and silenced with 3
455 different RNAi targeting *usp19* gene. **C:** Total cell extract of primary fibroblasts silenced for
456 *usp19* gene or overexpressing GFP-tagged USP19 revealed with GFP, LRP6 and Actin
457 antibodies. Quantification of LRP6 cellular amount is shown on the right. Errors represent
458 standard deviation (n=3) and *<p=0.05. **C:** Immunoprecipitation of transiently expressed
459 palmitoylation deficient myc-LRP6 (Myc-LRP6$^{CC\text{-}SS}$) upon *usp19* silencing. Quantification of
460 Myc-LRP6$^{CC\text{-}SS}$ cellular amount in TCE is shown on the right. Errors represent standard
461 deviation (n=3) and *<p=0.05. **D:** Immunoprecipitation of transiently expressed

462 palmitoylation deficient myc-LRP6 (Myc-LRP6^{CC-SS}) upon overexpression of GFP-tagged
463 USP19 vs. GFP-tagged USP19 (GFP-USP19) catalytically inactive mutant (GFP-USP19^{C506S}).
464
465 **Figure 4-figure supplement 1: *usp19* silencing leads to decrease in LRP6 cell surface**
466 **expression.** Surface Biotinylation assay performed in RPE1 cells upon 24, 48 and 72 hrs of
467 *usp19* or *usp13* gene silencing. Quantification of endogenous LRP6 surface expression at 48
468 hrs of gene silencing in Streptavidin-mediated pull down is shown above the western blot.
469 Errors represent standard deviation (n=3) and ***<p=0.0005.
470
471 **Figure 1-source data 1:** numeric data for graphs of figure 1B, 1D, 1E, 1F, and 1H
472
473 **Figure 2-source data 2:** numeric data for graphs of figure 2A, 2B, 2C, 2E and 2F
474
475 **Figure 3-source data 3:** numeric data for graphs of figure 3C, 3D, 3E and 3F
476
477 **Figure 4-source data 4:** numeric data for graphs of figure 4A and 4B
478
479 **Figure 1-suppl1-source data 1:** numeric data for graphs of figure 1 S1A
480
481 **Figure 3-suppl1-source data 1:** numeric data for graphs of figure 3 S1A and 3 S1C
482
483 **Figure 4-suppl1-source data 1:** numeric data for graphs of figure 4 S1
484

485 **REFERENCES**

486 Abrami, L., Kunz, B., Deuquet, J., Bafico, A., Davidson, G., and van der Goot, F.G. (2008a).
487 Functional interactions between anthrax toxin receptors and the WNT signalling protein
488 LRP6. Cellular microbiology *10*, 2509-2519.

489 Abrami, L., Kunz, B., Iacovache, I., and van der Goot, F.G. (2008b). Palmitoylation and
490 ubiquitination regulate exit of the Wnt signaling protein LRP6 from the endoplasmic
491 reticulum. Proceedings of the National Academy of Sciences of the United States of
492 America *105*, 5384-5389.

493 Altun, M., Zhao, B., Velasco, K., Liu, H., Hassink, G., Paschke, J., Pereira, T., and Lindsten,
494 K. (2012). Ubiquitin-specific protease 19 (USP19) regulates hypoxia-inducible factor
495 1alpha (HIF-1alpha) during hypoxia. J Biol Chem *287*, 1962-1969.

496 Brodsky, J.L., and Skach, W.R. (2011). Protein folding and quality control in the endoplasmic
497 reticulum: Recent lessons from yeast and mammalian cell systems. Curr Opin Cell Biol *23*,
498 464-475.

499 Clague, M.J., Barsukov, I., Coulson, J.M., Liu, H., Rigden, D.J., and Urbe, S. (2013).
500 Deubiquitylases from genes to organism. Physiological reviews *93*, 1289-1315.

501 Deuquet, J., Abrami, L., Difeo, A., Ramirez, M.C., Martignetti, J.A., and van der Goot, F.G.
502 (2009). Systemic hyalinosis mutations in the CMG2 ectodomain leading to loss of function
503 through retention in the endoplasmic reticulum. Human mutation *30*, 583-589.

504 Deuquet, J., Lausch, E., Guex, N., Abrami, L., Salvi, S., Lakkaraju, A., Ramirez, M.C.,
505 Martignetti, J.A., Rokicki, D., Bonafe, L., *et al.* (2011a). Hyaline Fibromatosis Syndrome
506 inducing mutations in the ectodomain of anthrax toxin receptor 2 can be rescued by
507 proteasome inhibitors. EMBO Mol Med *3*, 208-221.

508 Deuquet, J., Lausch, E., Superti-Furga, A., and van der Goot, F.G. (2011b). The dark sides of
509 capillary morphogenesis gene 2. The EMBO journal *31*, 3-13.
510 Ellgaard, L., McCaul, N., Chatsisvili, A., and Braakman, I. (2016). Co- and post-translational
511 protein folding in the ER. Traffic.
512 Feldman, M., and van der Goot, F.G. (2009). Novel ubiquitin-dependent quality control in the
513 endoplasmic reticulum. Trends in cell biology *19*, 357-363.
514 Guerriero, C.J., and Brodsky, J.L. (2012). The delicate balance between secreted protein
515 folding and endoplasmic reticulum-associated degradation in human physiology.
516 Physiological reviews *92*, 537-576.
517 Hassink, G.C., Zhao, B., Sompallae, R., Altun, M., Gastaldello, S., Zinin, N.V., Masucci,
518 M.G., and Lindsten, K. (2009). The ER-resident ubiquitin-specific protease 19 participates
519 in the UPR and rescues ERAD substrates. EMBO Rep *10*, 755-761.
520 Hsieh, J.C., Lee, L., Zhang, L., Wefer, S., Brown, K., DeRossi, C., Wines, M.E., Rosenquist,
521 T., and Holdener, B.C. (2003). Mesd encodes an LRP5/6 chaperone essential for
522 specification of mouse embryonic polarity. Cell *112*, 355-367.
523 Jin, S., Tian, S., Chen, Y., Zhang, C., Xie, W., Xia, X., Cui, J., and Wang, R.F. (2016). USP19
524 modulates autophagy and antiviral immune responses by deubiquitinating Beclin-1. The
525 EMBO journal.
526 Joiner, D.M., Ke, J., Zhong, Z., Xu, H.E., and Williams, B.O. (2013). LRP5 and LRP6 in
527 development and disease. Trends in endocrinology and metabolism: TEM *24*, 31-39.
528 Lamriben, L., Graham, J.B., Adams, B.M., and Hebert, D.N. (2016). N-Glycan-based ER
529 Molecular Chaperone and Protein Quality Control System: The Calnexin Binding Cycle.
530 Traffic *17*, 308-326.

531 Lee, J.G., Takahama, S., Zhang, G., Tomarev, S.I., and Ye, Y. (2016). Unconventional
532 secretion of misfolded proteins promotes adaptation to proteasome dysfunction in
533 mammalian cells. Nature cell biology.

534 Lemus, L., and Goder, V. (2014). Regulation of Endoplasmic Reticulum-Associated Protein
535 Degradation (ERAD) by Ubiquitin. Cells *3*, 824-847.

536 Li, J., Li, C., Liang, D., Lv, F., Yuan, T., The, E., Ma, X., Wu, Y., Zhen, L., Xie, D*., et al.*
537 (2016). LRP6 acts as a scaffold protein in cardiac gap junction assembly. Nature
538 communications *7*, 11775.

539 MacDonald, B.T., Tamai, K., and He, X. (2009). Wnt/beta-catenin signaling: components,
540 mechanisms, and diseases. Developmental cell *17*, 9-26.

541 Mei, Y., Hahn, A.A., Hu, S., and Yang, X. (2011). The USP19 deubiquitinase regulates the
542 stability of c-IAP1 and c-IAP2. J Biol Chem *286*, 35380-35387.

543 Riordan, J.R. (2008). CFTR function and prospects for therapy. Annual review of
544 biochemistry *77*, 701-726.

545 Wing, S.S. (2016). Deubiquitinating enzymes in skeletal muscle atrophy-An essential role for
546 USP19. The international journal of biochemistry & cell biology.

547 Xu, C., and Ng, D.T. (2015). Glycosylation-directed quality control of protein folding. Nat
548 Rev Mol Cell Biol *16*, 742-752.

549 Ye, Y. (2006). Diverse functions with a common regulator: ubiquitin takes command of an
550 AAA ATPase. J Struct Biol *156*, 29-40.

551

552

553

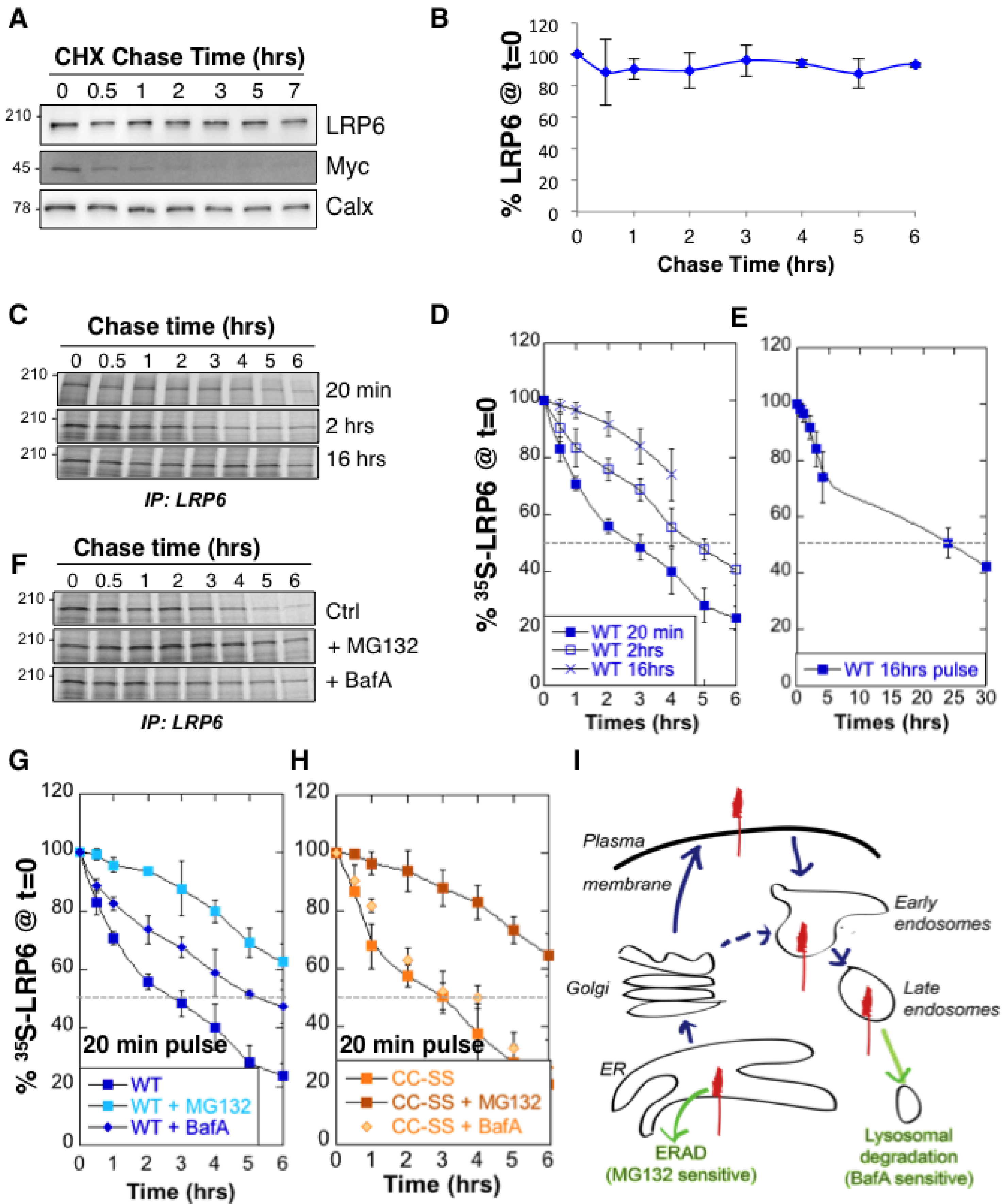
A
CHX Chase Time (hrs)
0 0.5 1 2 3 5 7
210
LRP6
45
Myc
78
Calx
B
% LRP6 @ t=0
Chase Time (hrs)
C
Chase time (hrs)
0 0.5 1 2 3 4 5 6
20 min
2 hrs
16 hrs
IP: LRP6
D
% 35S-LRP6 @ t=0
WT 20 min
WT 2hrs
WT 16hrs
Times (hrs)
E
WT 16hrs pulse
Times (hrs)
F
Chase time (hrs)
0 0.5 1 2 3 4 5 6
Ctrl
+ MG132
+ BafA
IP: LRP6
G
% 35S-LRP6 @ t=0
20 min pulse
WT
WT + MG132
WT + BafA
Time (hrs)
H
20 min pulse
CC-SS
CC-SS + MG132
CC-SS + BafA
Time (hrs)
I
Plasma
membrane
Early
endosomes
Golgi
Late
endosomes
ER
ERAD
(MG132 sensitive)
Lysosomal
degradation
(BafA sensitive)

Perrody, Abrami et al. Figure 2

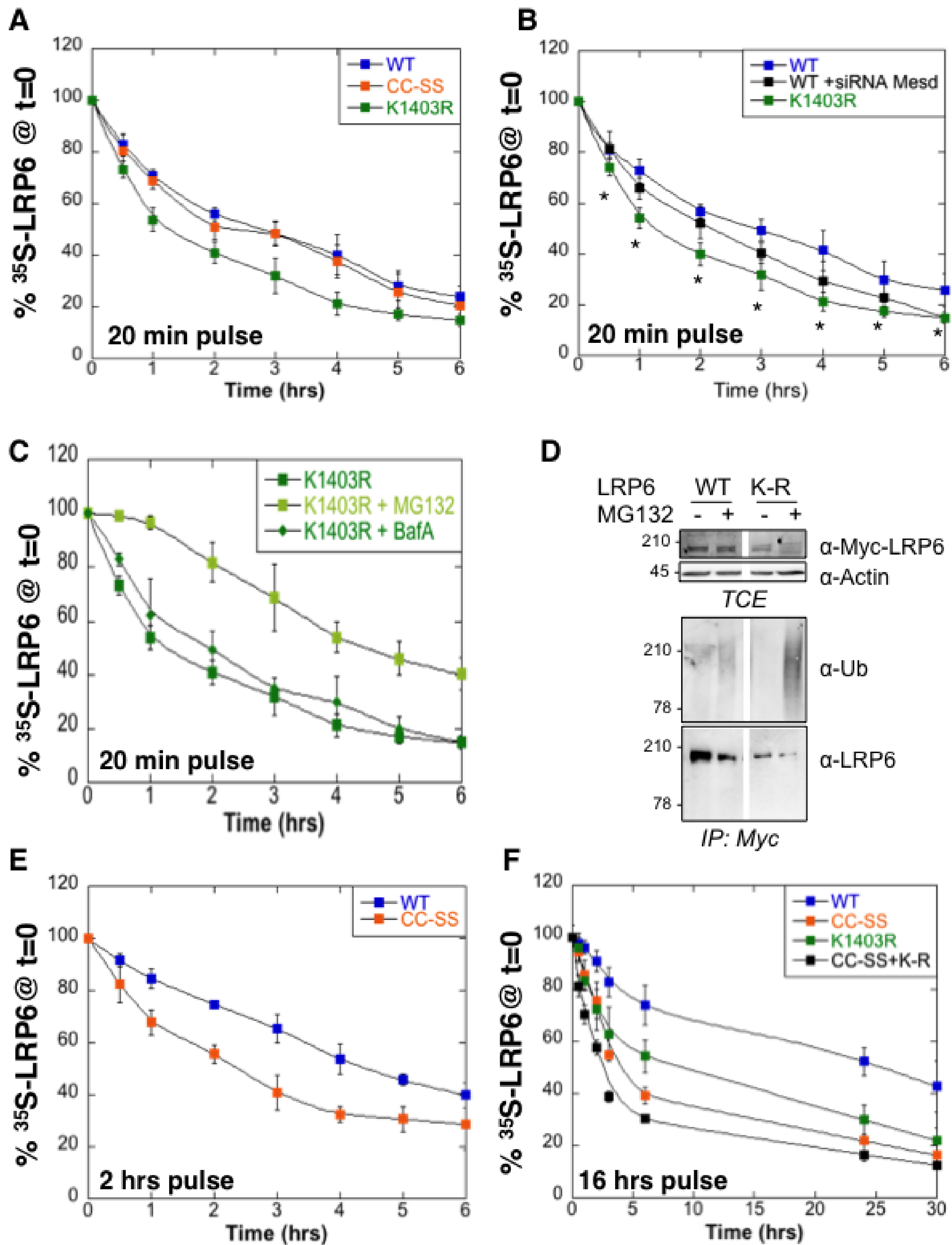

Perrody, Abrami et al. Figure 3

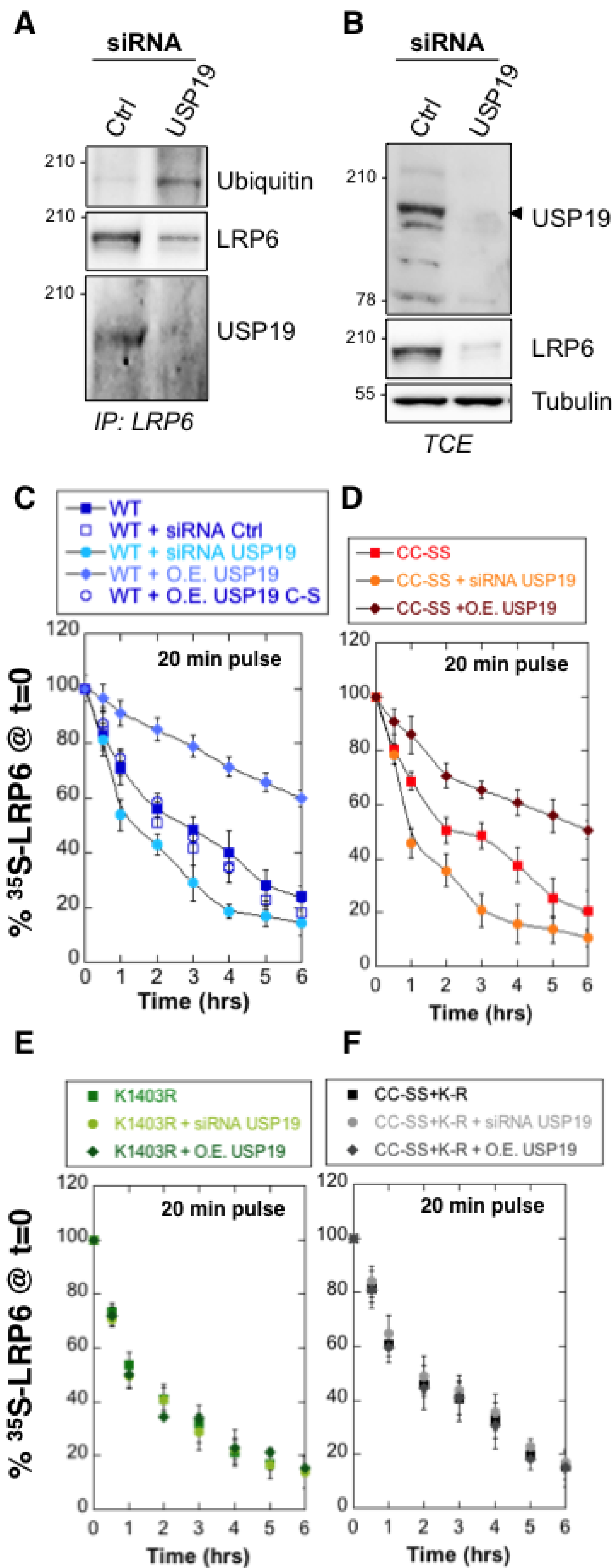

A

% of Wnt signaling

200
150
100
50
0

*

GFP-USP19 - - - - +
Myc-LRP6 - - + + +
Mesd - + - + +

B

% of Wnt signaing

120
100
80
60
40
20
0

Ctrl USP19 USP13

siRNA in RPE1

D

Ctrl siRNA
USP19
siRNA
O/E

210 LRP6
55 CMG2
78 55 TEM8
210 EGF-R
78 Tf-R
45 Actin

E

CFTR
USP19
-

210 CFTR
210 GFP-USP19
55 Tubulin

C

ER exit
mesd and other chaperones mediated folding
ER lumen
Cytosol
DHHC
-Lys-
-Cys-
-Cys-
-Lys-
-Lys-
-Lys-
E3 Ligase 1
USP19
-Cys-
-Cys-
-Lys-Ub
-Lys-
-Lys-
E3 Ligase 2
-Cys-
-Cys-
-Lys-Ub
-Lys-Ub-Ub-Ub
-Lys-Ub-Ub-Ub
ERAD
Synthesis

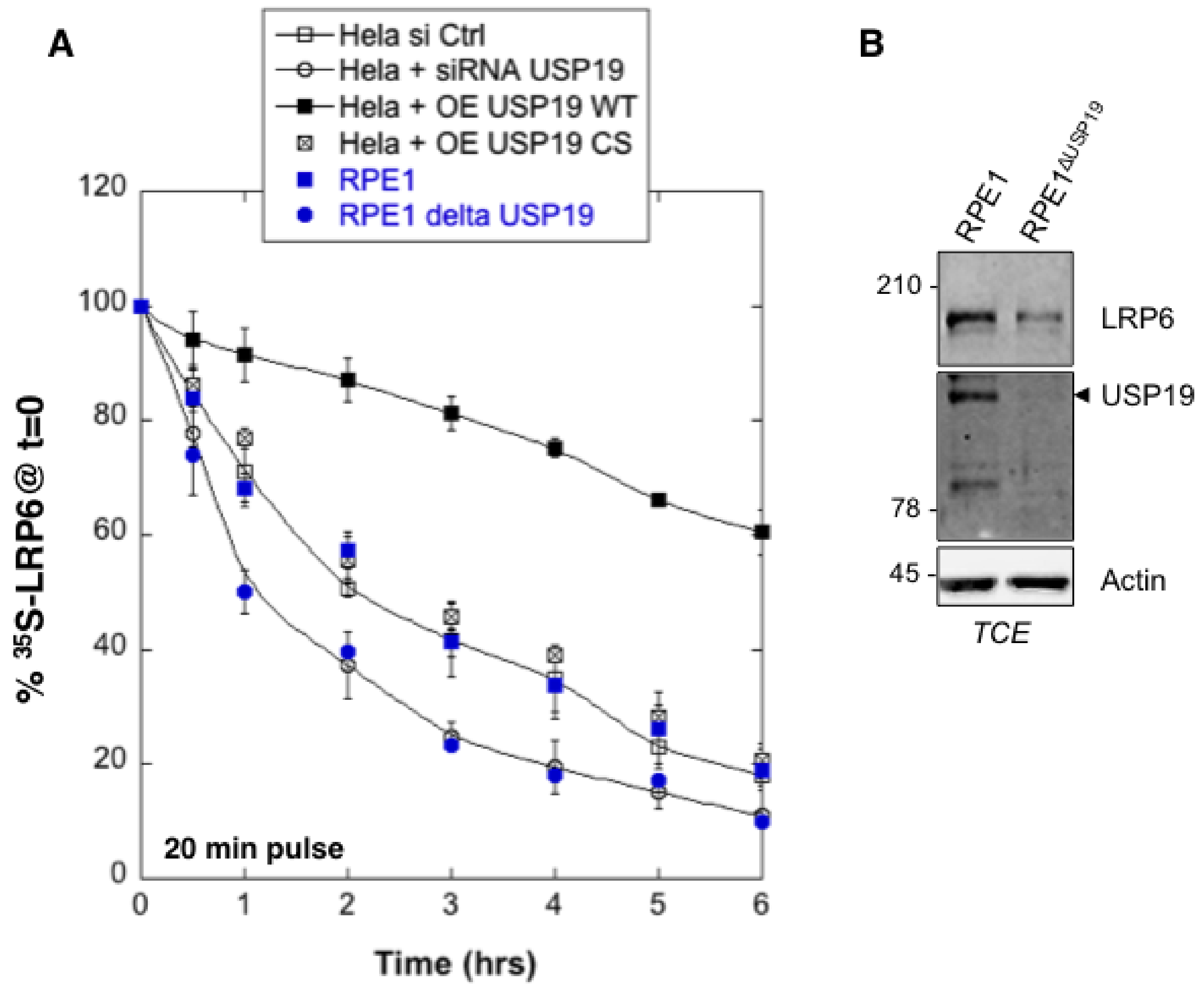
A
Hela si Ctrl
Hela + siRNA USP19
Hela + OE USP19 WT
Hela + OE USP19 CS
RPE1
RPE1 delta USP19
% 35S-LRP6@ t=0
20 min pulse
Time (hrs)
B
RPE1
RPE1ΔUSP19
210
78
45
LRP6
USP19
Actin
TCE

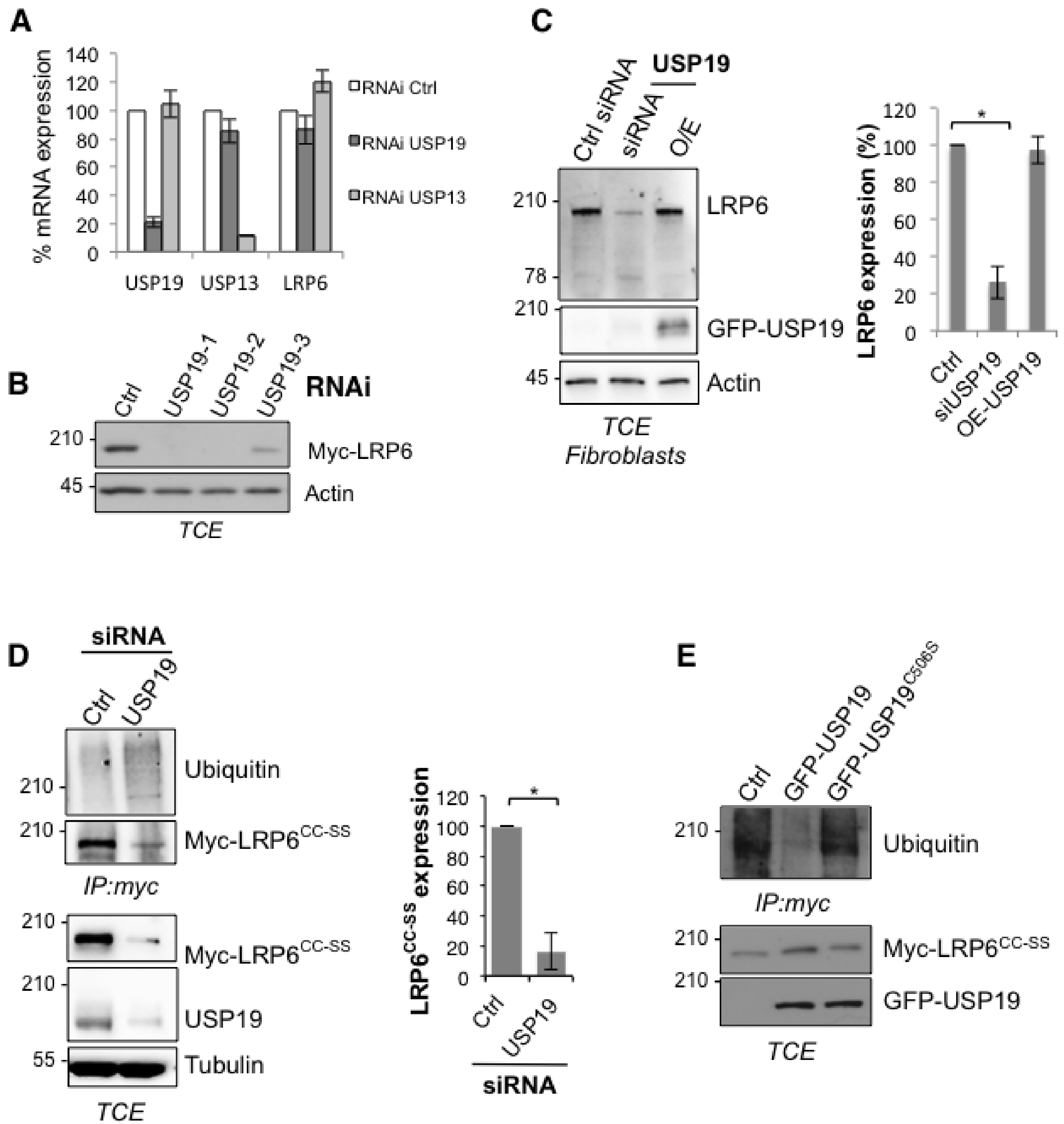
A
% mRNA expression
140
120
100
80
60
40
20
0
USP19
USP13
LRP6
RNAi Ctrl
RNAi USP19
RNAi USP13
B
Ctrl
USP19-1
USP19-2
USP19-3
RNAi
210
45
Myc-LRP6
Actin
TCE
C
Ctrl siRNA
siRNA
O/E
USP19
210
78
210
45
LRP6
GFP-USP19
Actin
TCE
Fibroblasts
LRP6 expression (%)
120
100
80
60
40
20
0
*
Ctrl
siUSP19
OE-USP19
D
siRNA
Ctrl
USP19
Ubiquitin
210
210
Myc-LRP6^{CC-SS}
IP:myc
210
Myc-LRP6^{CC-SS}
210
USP19
55
Tubulin
TCE
LRP6^{CC-SS} expression
120
100
80
60
40
20
0
*
Ctrl
USP19
siRNA
E
Ctrl
GFP-USP19
GFP-USP19^{C506S}
210
Ubiquitin
IP:myc
210
Myc-LRP6^{CC-SS}
210
GFP-USP19
TCE

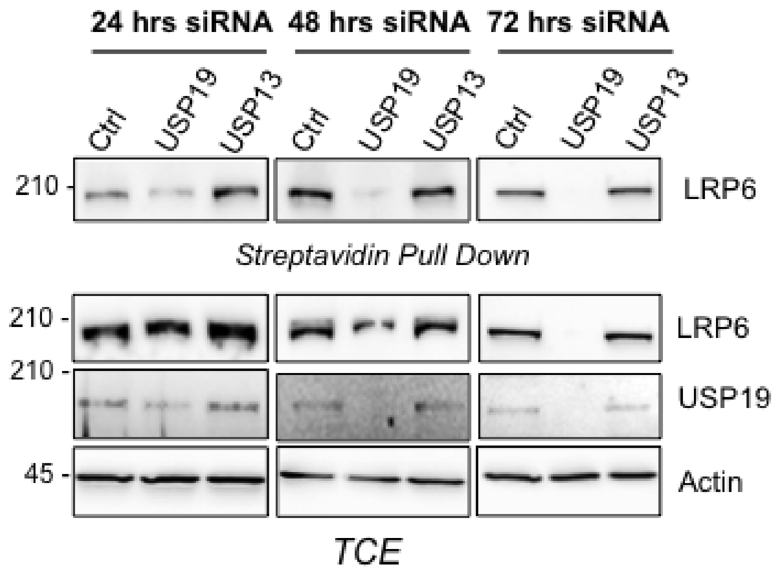
24 hrs siRNA
48 hrs siRNA
72 hrs siRNA
Ctrl
USP19
USP13
210
LRP6
Streptavidin Pull Down
210
LRP6
210
USP19
45
Actin
TCE

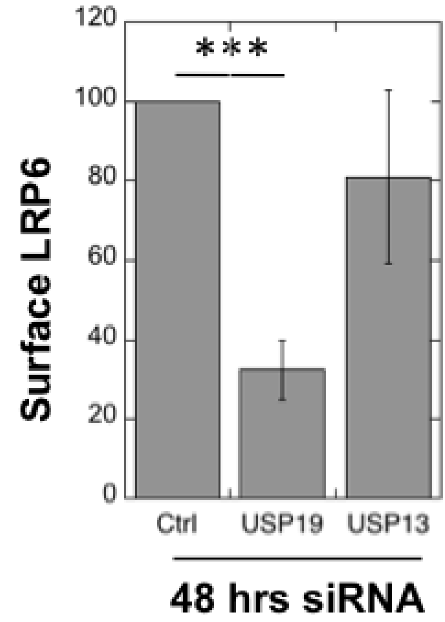
Surface LRP6
***
120
100
80
60
40
20
0
Ctrl
USP19
USP13
48 hrs siRNA